Noninvasive measurement of pulmonary transvascular protein flux in normal man.

A B Gorin, … , J Kohler, G DeNardo

J Clin Invest. 1980;66(5):869-877. https://doi.org/10.1172/JCI109953.

Research Article

Onset of lung edema is usually associated with increase in the pulmonary transvascular flux of water and proteins. Clinical measurement of these parameters may aid in early diagnosis of pulmonary edema, and allow differentiation between "cardiogenic" and "noncardiogenic" types base on the magnitude of the detected changes. We have previously described a noninvasive method for estimating transvascular protein flux in lung (Gorin, A. B., W. J. Weidner, R. H. Demling, and N. C. Staub, 1978. Noninvasive measurement of pulmonary transvascular protein flux in sheep. J. Appl. Physiol. 45: 225-233). Using this method we measured the net transvascular flux of [113mIn]transferrin (mol wt, 76,000 in lungs of nine normal human volunteers. Plasma clearance of [113In]transferrin occurred with a T1/2 = 7.0 +/- 2.6 h (mean +/- SD). The pulmonary transvascular flux coefficient, alpha, was 2.9 +/- 1.4 X 10(-3) ml/s (mean +/- SD) in man, slightly greater than that previously measured in sheep (2.7 +/- 0.7 X 10(-3) ml/s; mean +/- SD). The pulmonary transcapillary escape rate is twofold greater than the transcapillary escape rate for the vascular bed as a whole, indicating a greater "porosity" of exchanging vessels in the lung than exists for the "average" microvessel in the body. Time taken to reach half-equilibrium concentration of tracer protein in the lung interstitium was quite short, 52 +/- 13 min […]

Noninvasive Measurement of Pulmonary Transvascular Protein Flux in Normal Man

ARNOLD BERNARD GORIN, JAMES KOHLER, and GERALD DENARDO,
Departments of Internal Medicine and Nuclear Medicine, University of California, Davis, and the Cardiovascular Research Institute, University of California, San Francisco, California 94102

ABSTRACT Onset of lung edema is usually associated with increase in the pulmonary transvascular flux of water and proteins. Clinical measurement of these parameters may aid in early diagnosis of pulmonary edema, and allow differentiation between "cardiogenic" and "noncardiogenic" types based on the magnitude of the detected changes. We have previously described a noninvasive method for estimating transvascular protein flux in lung (Gorin, A. B., W. J. Weidner, R. H. Demling, and N. C. Staub. 1978. Noninvasive measurement of pulmonary transvascular protein flux in sheep. *J. Appl. Physiol.* **45:** 225–233). Using this method, we measured the net transvascular flux of [^{113m}In]transferrin (mol wt, 76,000) in lungs of nine normal human volunteers.

Plasma clearance of [^{113}In]transferrin occurred with a $T_{1/2}$ = 7.0±2.6 h (mean±SD). The pulmonary transvascular flux coefficient, α, was 2.9±1.4 × 10^{-3} ml/s (mean ±SD) in man, slightly greater than that previously measured in sheep (2.7±0.7 × 10^{-3} ml/s; mean±SD). The pulmonary transcapillary escape rate is twofold greater than the transcapillary escape rate for the vascular bed as a whole, indicating a greater "porosity" of exchanging vessels in the lung than exists for the "average" microvessel in the body. Time taken to reach half-equilibrium concentration of tracer protein in the lung interstitium was quite short, 52±13 min (mean±SD).

We have shown that measurement of pulmonary transvascular protein flux in man is practical. The coefficient of variation of measurements of α (between subjects) was 0.48, and of measurements of pulmonary transcapillary escape rates was 0.39. In animals, endothelial injury commonly results in a two- to threefold increase in transvascular protein flux. Thus, external radioflux detection should be a suitable means of quantitating lung vascular injury in human disease states.

INTRODUCTION

The water capacitance of the lung always exceeds its normal water content. Considerable increase in extravascular lung water can occur before flooding of alveoli results in disturbance of respiratory gas exchange (1). During this period of interstitial water filling, detection of pulmonary edema would allow early and aggressive therapy before the appearance of significant clinical symptoms.

Onset of lung edema is usually associated with increase in the pulmonary transvascular flux of water and proteins. In typical "cardiogenic" pulmonary edema, recruitment of capillary bed results in an increased surface area available for macromolecular flux, whereas an increase in convective forces leads to greater flux per unit surface area (2–4). In "noncardiogenic" pulmonary edema, a "capillary-leak syndrome," with impairment of the normal molecular sieving function of the endothelial membrane, results in veritable "flooding" of the interstitium with oncotically active proteins (5–7). Clinical measurement of transvascular protein flux in lung may aid in early diagnosis of pulmonary edema, and allow differentiation between "cardiogenic" and "noncardiogenic" types based on the magnitude of detected changes.

We have previously described a noninvasive method for estimating transvascular protein flux in the lung (8). The validity and sensitivity of this technique, external radioflux detection, was demonstrated by comparing our indirect assessment of interstitial accumulation of tracer protein with the directly measured accumulation in lung lymph of sheep. We now report values for pulmonary transvascular protein flux measured by external

Address reprint requests to Dr. Gorin, Section of Pulmonary Medicine, Department of Internal Medicine, Houston Veterans Administration Hospital, Baylor University School of Medicine, Houston, Texas.

Received for publication 7 January 1980 and in revised form 2 June 1980.

radioflux detection in normal human volunteers under base-line conditions.

GLOSSARY OF SYMBOLS

α	Pulmonary transvascular flux coefficient
α_T	Whole lung transvascular flux coefficient
β'	Rate constant-return of solute from extravascular to vascular compartment
CRT	Cathode-ray tube
D	Labeled protein tracer
D_{EVe}	Expected contribution to externally derived count rate by the fraction of D in EV compartment
D_{IVe}	Expected contribution to externally detected count rate by the fraction of D in IV compartment at any time
D_{ti}	Externally detected total count rate for *D*
D_{WB}	Observed count rate for D in a venous sample drawn at any time
EV	Extravascular lung compartment
EVe	Expected count rate from pulmonary interstitum
IV	Intravascular lung compartment
IVe	Expected count rate from vascular compartment
K	Constant correction factor
κ'	Time constant
PBV_r	Regional pulmonary blood volume
PPV	Pulmonary plasma volume
R	Marker restricted to IV compartment
RBC	Erythrocytes
R_{WB}	Observed count rate for R in a venous sample drawn at any time
TCER	Transcapillary escape rate
t_e	Time to reach maximum tracer concentration in the lung interstitum
[^{113}In]Tf	[^{113}In]Transferrin
t_i	Any time
t_0	Time zero
$t_{1/2}$	Time to reach half-maximum tracer concentration in the pulmonary interstitum
Vc	Pulmonary capillary blood volume
V_{IS}	Intersital volume of distribution of D
WB	Venous whole blood sample

METHODS

External radioflux detection. In a simple lung model there are two compartments (intravascular [IV] and extravascular [EV]). A labeled protein tracer (D) introduced in the IV compartment will, in time, be partitioned between both. Transport may be bidirectional, but net flux is along a concentration gradient. (However, no change in the steady-state osmotic force exerted by the tracer molecule occurs in either compartment because of the very low tracer concentrations used.) The flux between compartments occurs at a rate far in excess of that for metabolic degradation in either, and a dynamic equilibrium is eventually reached.

A scintillation detection unit (probe) externally positioned over the lung must measure input from tracer in both compartments; a venous sample of whole blood (WB) taken simultaneously and counted in a well counter will measure input only from one (IV). By also using a marker restricted to the IV compartment (R) it is possible to partition the probe input by use of the following relationship.

$$\frac{D_{IVe}\ \text{(counts per minute/field)}}{D_{WB}\ \text{(counts per minute/milliliter)}} = \frac{R_{IV}\ \text{(counts per minute/field)}}{R_{WB}\ \text{(counts per minute/milliliter)}} \times K, \quad (1)$$

where D_{IVe} is the expected contribution to the externally detected count rate by that fraction of the diffusible label in the IV compartment at any time, (t_i); D_{WB} is the observed count rate for that label in a venous sample drawn at t_i; R_{IV} is the externally detected count rate for the restricted label at any time, t_i; R_{WB} is the observed count rate for that label in a venous sample drawn at t_i; K, a constant correction factor.

Eq. 1 is an identity stating that there is a regional pulmonary blood volume (milliliters/field), which may be measured externally using any isotopes, so long as we correct for the results of differing photon energies.

The externally detected total count rate for the diffusible indicator (D_{t_i}) is:

$$D_{t_i} = D_{IVe} + D_{EVe}, \quad (2)$$

where D_{EVe} is the contribution to the externally detected count rate by that fraction of the diffusible label in the EV compartment at t_i (counts per minute/field).

At time zero (t_0) when no flux from IV to EV compartment for D has yet occurred, $D_{EV_e} = 0$, and $D_{ti} = D_{IVe}$. The value for K is thus obtained from experimental data at t_0.

K includes several elements. The differing energies of the two radiolabels result in differing tissue penetrance (i.e., the volume of tissue sampled by the detector increases with the energy of the gamma ray), and a differing counting efficiency of the detectors for each isotope. The IV compartment is itself partitioned, and D and R are restricted to separate subcompartments of unequal volume (i.e., plasma and erythrocyte (RBC) space). Any differences between large vessel and organ hematocrits is also included. Since the density and geometry of the thorax are constant in any given experiment but vary from subject to subject, the ability to derive K empirically in each experiment is very important.

Using Eqs. 1 and 2, we detect the increase in the extravascular mass of diffusible tracer protein in lung over time. Mathematical analysis of the rate of increase will yield a transvascular transfer coefficient.

Subjects. Measurements were made in nine normal males, age 22–34 yr. All were nonsmokers. Five subjects were studied again, after an interval of at least 6 mo. The maximum absorbed radiation dose to the volunteer in any one study was 230 mrad. Protocols were approved by both the Radioisotope Use Committee and Human Subjects (clinical) Committee of the University of California Davis Medical Center. Informed consent was obtained in all cases.

Radiopharmaceuticals. Autologous RBC were labeled with ^{99m}Tc (half-life, 6 h) by the method of Korubin et al. (9). Heparinized plasma, saved from the initial cell separation, was labeled in vitro with ^{113m}In (half-life, 100 min) by dropwise addition to the sterile eluate of an Indium generator (New England Nuclear, Boston, Mass.). Indium binds with high specificity to transferrin, a β-globulin (mol wt, 76,000). All agents were prepared using aseptic techniques in the

radiopharmacy of the Nuclear Medicine Section, University of California Davis Medical Center.

Protocol. Subjects were studied supine. A scintillation detection probe was positioned over the right midlung field (~T-6 level) or the left lung apex (~T-4 level). 3–5 mCi of autologous ^{99m}Tc-RBC were given as an intravenous bolus and 10 min was allowed for dispersion in the vascular space. We then gave 5–10 mCi autologous [^{113m}In]transferrin ([^{113m}In]Tf) as a bolus injection at the same site (t_0). An intravenous heparin lock was placed in the opposite arm and 3-ml WB were drawn at 10-min intervals during the next 60 min. Sequential 50-s counts of gamma emissions from both isotopes were made over the lung for periods of 60–90 min.

Special instrumentation. We performed these studies using any one (or two) of three different scintillation detection probes: (*a*) 3 × 2 in. NaI crystal (Nuclear Chicago, Des Plaines, Ill.), fitted with a multi-hole collimator focused to a field 4 cm Diam at a point 14 cm from the collimator face (8, complete description of collimator response); (*b*) 2 × 2 in. NaI crystal (Nuclear Chicago) fitted with a single-channel, diverging collimator (two of these units were available); (*c*) 2 × 2 in. NaI crystal (ADAC Laboratories, Sunnyvale, Calif.), fitted with a single-channel, (2 in. Diam) parallel wall collimator.

The signal output from the probes was processed by a computer-based multichannel-analyzer (TN-11 system, Tracor/Northern, Middleton, Wis.). Thus, we were able to continuously sample the entire spectrum of photon energies between 0 and 1,000 keV. During the 50-s counting periods, accumulating γ-emissions were displayed on a 6 in. cathode-ray tube (CRT) screen. Two peaks, representing the monoenergic photons of ^{99m}Tc (140 keV) and ^{113m}In (390 keV), are clearly seen to emerge above background radiation (Fig. 1). At the end of each 50-s interval of data acquisition, background radiation was stripped from the data, the area under the upper peak (^{113m}In emissions) integrated, the ^{113m}In emissions (including Compton scattered radiation) stripped from the data, and the area under the lower peak (^{99m}Tc emissions) integrated (Fig. 1). Stripping was accomplished by reference to spectra (background and pure ^{113m}In) obtained before administration of the radiopharmaceuticals and stored on floppy disk. ^{113m}In and ^{99m}Tc count rates were then corrected for radioactive decay to equivalent count rates at t_0. These operations were performed automatically by a PDP 11/10 computer, 32K core (Digital Equipment Corp., Marlboro, Mass.) around which the TN-11 system is assembled. The corrected count rates, real time of data acquisition, and time elapsed from t_0 were then simultaneously stored in computer memory and printed via an ASR-33 teletype terminal (Teletype Corp., Skokie, Ill.). The sequence of data acquisition and processing took between 1.5 and 2.5 min.

At the end of each study, all data points for each radiotracer over time could be displayed on the CRT screen (Fig. 2). Radioactivity of the patient's WB was then determined using a NaI well counter. The output signal of this unit was also processed by the multichannel analyzer in a fashion identical to that used for the signal from the external probes.

Data analysis. We weighed the WB counted in the well counter, determined the hematocrit of the sample, and expressed ^{113m}In activity as counts per minute per gram plasma. The decrease in plasma concentration of diffusible tracer over the time of the study is well fit by an exponential regression:

$$[^{113}\text{In-Tf}]_{t_i} \text{ (counts per minute/gram)} = [^{113}\text{In-Tf}]_{t_0} \text{ (counts per minute/gram)}\, e^{-\kappa' t} \quad (3)$$

The time constant (κ') a function of the plasma clearance of the diffusible tracer protein, is frequently called the "transcapillary escape rate" (TCER) (10).

^{99m}Tc activity in whole blood falls slowly as RBC damaged in the labeling procedure are sequestered in the spleen, and the radiolabel elutes from the RBC. The ratio of ^{113m}In activity to ^{99m}Tc activity in whole blood is a decreasing monotonic function (Fig. 3). Again, the data is well fit by an exponential regression:

$$\frac{^{113m}\text{In}_{WBt_i} \text{ (counts per minute/gram)}}{^{99m}\text{Tc}_{WBt_i} \text{ (counts per minute/gram)}} = a e^{-xt_i}, \quad (4)$$

where $a = D_{WB}/R_{WB}$ at t_0.

In these studies, the externally detected count rate for ^{99m}Tc over lung either remained constant, or fell slightly over time, reflecting a decrease in regional pulmonary blood volume. The rate of macromolecular efflux from the pulmonary microcirculation is relatively greater than that from the vascular compartment as a whole (11, 12). Thus, the concentration of [^{113m}In]Tf rises more rapidly in the lung interstitium than it falls in the vascular space, and the externally detected count rate for ^{113m}In over lung increases during the course of the

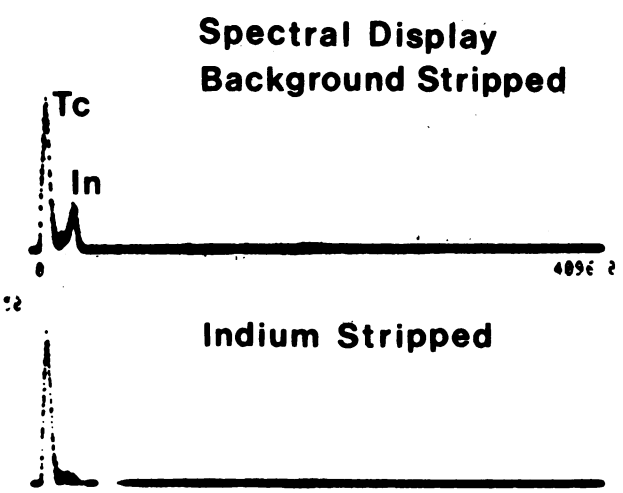

FIGURE 1 Polaroid photograph of CRT screen, TN-11 multichannel analyzer (Tracor/Northern), after 50 s accumulation of γ-emissions during typical study. In upper panel, background radiation has been stripped from spectrum showing monoenergic peaks of ^{113m}In (390 keV) and ^{99m}Tc (140 keV). In the lower panel, the ^{113m}In spectrum, including Compton scatter, has been stripped from the display, leaving only the ^{99m}Tc peak.

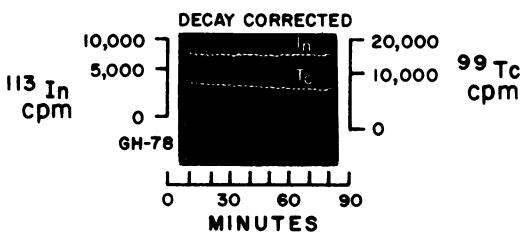

FIGURE 2 Polaroid photograph of CRT screen, TN-11 multichannel analyzer (Tracor Northern) showing ^{113m}In and ^{99m}Tc counts during sequential 50-s intervals in an 80-min study (log scale). Counts have been corrected for isotopic decay to equivalent counts at t_0.

study. The ratio of the externally detected count rate for ^{99m}Tc to ^{113m}In over time is also a decreasing monotonic function (Fig. 3) and, again,

$$\frac{^{99m}\text{Tc}_{t_i}\ (\text{counts per minute/field})}{^{113m}\text{In}_{t_i}\ (\text{counts per minute/field})} = be^{-zt_i}, \qquad (5)$$

where $b = R_{IV}/D_{IVe}$ at t_0.

Thus, the correction factor in Eq. 1 (K) = 1/(ab).

We use the empirically derived values of K and Eq. 4 to determine the expected value of D_{IV} at t_i, by substitution in Eq. 1,

$$D_{IVe}\ (\text{counts per minute/field}) = {}^{99m}\text{Tc (counts per minute/field)} \times Kae^{-xt_i} \qquad (6)$$

Thus we are able to partition the externally detected γ-emissions from the diffusible tracer protein into D_{IVe} and D_{EVe} pools.

Fig. 4 shows the change in D_{IVe} and D_{EVe} over time in a typical study. IVe falls at a rate exceeding plasma clearance, indicating an observed decrease in regional pulmonary blood volume over the course of the study (from ^{99m}Tc-RBC data). The mass of diffusible tracer protein in the EV compartment (proportional to EVe) increases over time. A line of best fit for this data has been drawn using the relationship:

$$D_{EVe} = \frac{\alpha[D_{IVe}]_{t_0}}{\beta' - \kappa'}(e^{-\kappa' t_i} - e^{-\beta' t_i}), \qquad (7)$$

where α = general transport coefficient governing solute flux (both convective and diffusive) from IV to EV space (volume/time per field); β' = rate constant governing return of solute from extravascular to vascular compartment (time^{-1}); κ' = TCER, defined by Eq. 3; and $[D_{IVe}]_{t_0}$ = the concentration of diffusible tracer protein in plasma at t_0 (counts per minute/gram plasma).

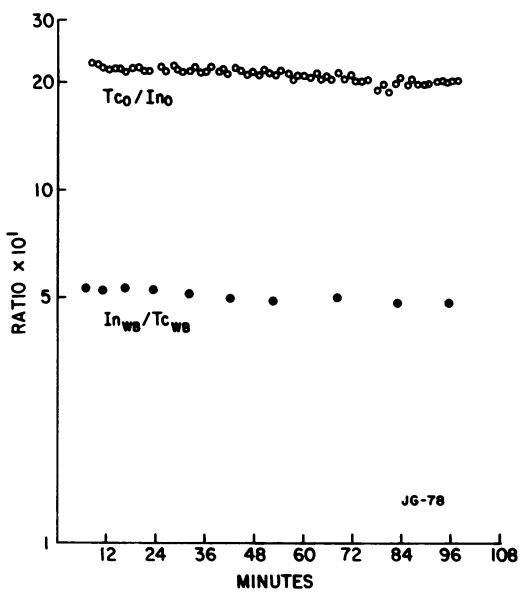

FIGURE 3 Ratios of externally detected emissions of ^{113m}In and ^{99}Tc from lung (Tc_0/In_0), and activity of these isotopes in whole blood (In_{WB}/Tc_{WB}) over time (log scale). It is obvious that these plots will be well fit by an exponential regression.

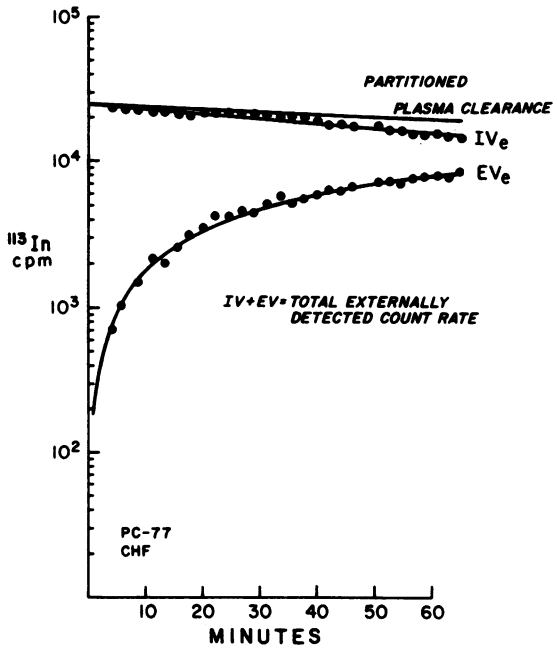

FIGURE 4 Total externally detected count rate for the diffusible protein tracer [^{113m}In]Tf from lung, partitioned using Eqs. 1 and 2 (Methods) and plotted over time. IVe is based on plasma clearance determined from venous blood samples and measured change in pulmonary blood volume determined using ^{99m}Tc-RBC. EVe rise over time. The line of best fit for EVe was determined using a minimum dispersion method and a two-compartment model of protein exchange (Eq. 7; Methods).

The derivation of Eq. 7 is given in a previous publication (8).[1] The compartmental system used is schematized in Fig. 5. Note that here β is the general transport coefficient governing flux of solute from the EV to the IV space. $\beta = \beta' V_{Is}$, where V_{Is} is the interstitial volume of distribution of the solute (β, volume/time).

In each study, we wish to solve Eq. 7 for the unknowns, α and β'. Values for the constants κ' and $[D_{IVe}]_{t_0}$ are available from Eq. 3. In any one study, we have between 20 and 35 measurements of D_{EVe} made over time. We can thus establish an extended set of simultaneous equations to solve for the two parameters, α and β'. The method of least squares (13) can be used to seek best estimates of the two coefficients (α and β' are both varied by the computer). It has been simpler to write a program in which the value of β' is estimated, and the value of α is then calculated at each time, t_i, using the corresponding value of EVe. The computer varies the estimate of β', seeking to minimize the dispersion in the values of α calculated across the set of simultaneous equations. There can also be no trend (increasing or decreasing) in the calculated values of α over time. The estimates of α and β' reached in this way exactly equal those reached by the least squares method. The coefficient of variation for the calculated values of α provides a measure of the scatter of data (values of EVe) around the line of best fit.

[1] Equation 14 in reference 8 is written incorrectly due to omission of brackets and an integral sign. The correct form is:

$$L = e^{-t}\left[\ C + \alpha[P]_{t_0} \int e^{(\beta-\kappa)t} dt\ \right].$$

The first derivative of Eq. 7 will equal zero when no net exchange of tracer protein occurs between IV and EV compartments. At that time, the lung interstitial concentration of tracer protein will be at its maximum value, and thereafter will decline along a single exponential. The time taken to reach maximum tracer concentration in the lung interstitium (t_e) is given by

$$t_e = \frac{\ln \beta'/\kappa'}{\beta' - \kappa'} \quad (8)$$

Insertion of t_e for t_i in Eq. 7 allows us to calculate the value of D_{EVe} at t_e. Eq. 7 can then be used to determine time to half-maximum tracer concentration in the pulmonary interstitium ($t_{1/2}$).

Whole lung values. The scintillation detection probes used in these studies all had a collimated field of view, and so detected γ-emissions from only a fraction of the total lung mass. Thus, the absolute value of α is highly idiosyncratic and depends upon the characteristics of the scintillation detection system and the tissue traversed by γ-emissions. The volume of lung sampled varied from probe to probe, and with placement of any given probe ([8] and see below for discussion of the effect of including nonlung tissue in the sampled field). Pulmonary transvascular protein flux, α, is a function of both vascular permeability and the surface area available for macromolecular exchange. The exchanging surface area should vary directly with the volume of lung tissue in the collimated field. Therefore, measurements of α made with two different probes, or even with the same probe on two different occasions, are not directly comparable unless normalized in some manner for the volume of tissue sampled in the study.

As the volume of lung tissue in the field varies, the regional pulmonary blood volume (PBV_r) also increases or decreases. Thus, data obtained using highly focused and widely open collimators can be compared by dividing α (milliliters/time) by PBV_r (milliliters). α/PBV_r ($time^{-1}$) is a time constant. If regional pulmonary plasma volume (PPV_r) is used in the denominator, rather than PBV_r, the resulting time constant is a pulmonary TCER comparable to TCER.

In any study, subtracting measured D_{EVe} from D_{IVe} at each t_i (analagous to subtracting lymph from plasma concentrations of diffusible tracer) yields a monotonic decreasing exponential function (Fig. 6). If the rate of exchange of diffusible tracer between IV and EV compartments in the core of tissue sampled by the external detector is representative of that

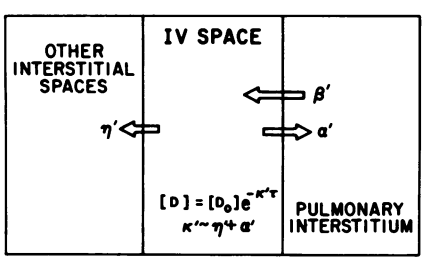

FIGURE 5 Schematic of the compartmental system within which tracer protein exchange has been analyzed in these studies. α' (α/PPV_r, the pulmonary transcapillary escape rate) and β' (β/V_{IS}) are time constants governing solute flux between vascular and extravascular spaces in the lung. η' is the time constant governing solute flux from vascular to extravacular spaces in nonlung tissue. κ' is the transcapillary escape rate. [D] is the concentration of the diffusible tracer in the IV compartment.

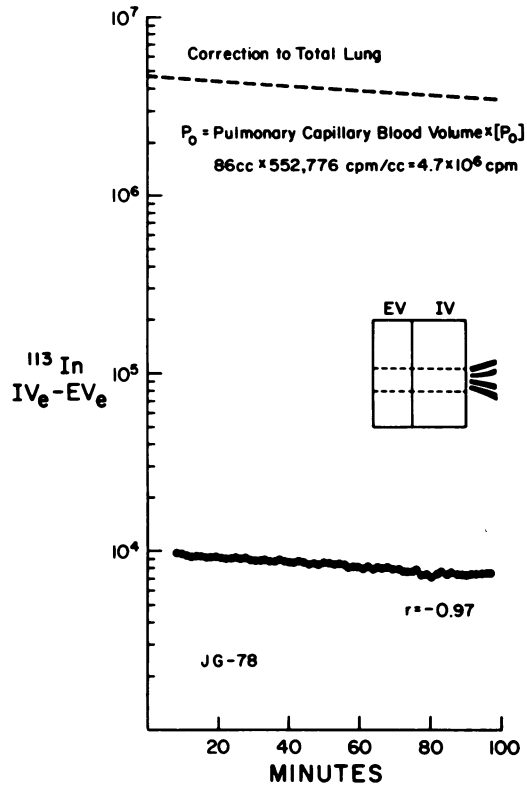

FIGURE 6 Subtraction of measured EVe from measured IVe over time (log scale). It is obvious that data is well fit by a monoexponential regression, suggesting a simple two-compartment equilibration. Data is obtained from a small core of lung tissue using a collimated detector. If this core is typical of all lung tissue, observations can be extended to the whole organ by determining P_0, IVe at t_0, in the total exchanging vascular volume of the lung.

throughout the lung, we can extrapolate from our regional data to whole lung values of $\alpha(\alpha_T)$. In the whole lung, the slope of $IV_e - EV_e$ over time will be the same as in the region we are sampling, but the intercept at t_0 will equal the mass of diffusible tracer in the exchanging vessels of the entire lung at t_0. We assumed that this whole lung intercept value was equal to the activity in blood at t_0 (known from the whole blood samples) multiplied by the pulmonary capillary blood volume (Vc) measured by the method of Roughton and Forster (14) (Fig. 6).

RESULTS

Data from 14 studies are shown in Tables I and II. In three studies, indicated by parentheses in the tables, the computer was unable to find a unique solution for β'. This will occur when the line of best fit for measured values of D_{EVe} is a linear regression. α will then be approximated by the slope of this line. Alternatively, β' and α can be estimated graphically from a plot of D_{IV}-D_{EVe}. If $D_{IV_{t_i}}$ is chosen so that:

$$D_{IV_{t_i}} = [D_{IVe}]_{t_0} V p e^{-\kappa' t_i}, \quad (9)$$

TABLE I

Parameters Describing Transvascular Protein Flux in Normal Man

Subject	α_T	α/PPV	Dispersion index*	β'	κ'	r_κ‡
	ml/h	$\times 10^{-3} min^{-1}$		$\times 10^{-3} min^{-1}$		
1a	8.1	2.69	0.3001	17.65	2.35	−0.97
b	8.5	2.85	0.2431	10.11	2.00	−0.97
2a	13.5	5.32	0.1305	7.27	1.88	−0.90
b	12.5	5.26	0.2180	8.78	1.31	−0.97
3a	8.9	6.71	0.1263	6.01	2.10	−0.99
b	8.8	(3.43)	—	(5.79)	1.76	−0.94
4a	4.9	(2.11)	—	(4.79)	2.11	−0.96
b	6.5	2.78	0.1559	5.56	2.89	−0.95
5a	8.4	5.23	0.3260	14.62	1.35	−0.97
b	16.2	4.27	0.1613	6.50	0.82	−0.99
6	24.8	5.38	0.1120	8.95	1.57	−0.87
7	10.1	3.37	0.1200	7.97	2.31	−0.95
8	11.3	(4.46)	—	(8.46)	1.82	−0.93
9	6.2	2.32	0.3444	11.52	1.34	−0.95
mean	10.6	3.80		8.86	1.83	
±SD	5.1	1.44		3.65	0.53	

Parentheses indicate three studies in which the computer was unable to find a unique solution for β'.

* The dispersion index is the coefficient of variation of values of α calculated for each t_i using real values of EVe and the reported values of β' and κ'. The mean value of α is used in calculating α/PPV_r.

‡ r_κ is the regression coefficient for values of [^{113m}In]Tf in plasma over time.

a restatement of Eq. 3 in which both sides of the equation have been multiplied by regional plasma volume (Vp), then

$$D_{IV_{t_i}} - D_{EVe_{t_i}} = [D_{IVe}]_{t_0} Vp e^{-wt_i}. \quad (10)$$

By definition, $[D_{IVe}]_{t_0} Vp = D_{IV_{t_0}}$, the mass of diffusible tracer in the field of the probe at t_0. Subtracting Eq. 10 from Eq. 9, we obtain

$$D_{EVe_{t_i}} = [D_{IVe}]_{t_0} Vp(e^{-\kappa' t} - e^{-wt}). \quad (11)$$

But
$$D_{EVe_{t_i}} = [D_{IVe}]_{t_0} \frac{\alpha}{\beta' - \kappa'} (e^{-\kappa' t_i} - e^{-\beta' t_i}). \quad (7)$$

Thus,
$$Vp(e^{-\kappa' t} - e^{-wt}) = \frac{\alpha}{\beta' - \kappa'} (e^{-\kappa' t_i} - e^{-\beta' t_i}). \quad (12)$$

$$\text{If } w \simeq \beta', \text{ then } Vp(w - \kappa') = \alpha. \quad (13)$$

This latter technique was used to estimate the bracketed values of α, β' and $t_{1/2}$ entered in Tables I and II.

In Fig. 7, we compare values of α/PPV obtained by the iterative process and by graphic solution in the other 11 studies. In normal man, the graphic method yields a good approximation of α. Unfortunately, this simple alternative yields a poor estimate of β' (β' graph = 7.685 × 10 − 0.210 computer; $r = -0.44$; Discussion).

After administration of [^{113m}In]Tf as an intravenous bolus, some finite time is required for uniform dispersion of the tracer in the vascular space (mixing time). During this early period, [^{113}In]Tf activity in peripheral venous samples may not reflect activity in the central blood volume. Drawing two or three samples at 3-min intervals after the bolus administration of [^{113m}In]Tf, we empirically found that the mixing phase lasted between 5 and 7 min in our subjects. Therefore, counts detected over the lung during the first 7 min after tracer injection were not used in estimating parameters. Vc = 73±8 cm^3 (mean±SD) in the nine subjects.

DISCUSSION

We have measured pulmonary transvascular protein flux in normal man using a noninvasive method, external radioflux detection. No previous assessments, direct or indirect, of this parameter have been reported in man. In an earlier publication (8), we demonstrated the validity and sensitivity of this technique by correlating our noninvasive determination of interstitial accumulation of tracer protein with the directly measured accumulation in lung lymph of sheep.

The estimates of TCER (κ') and time to reach one-half the value at time zero ($t_{1/2}$) for plasma [^{113m}In]Tf,

TABLE II
Equilibration of [^{113m}In]Tf between Vascular and Interstitial Compartments

Subject	Plasma clearance* $T_{1/2}$	Maximum lung interstitial tracer concentration‡ $t_{1/2}$
	min	
1a	295	27.1
b	347	42.8
2a	369	54
b	530	53
3a	330	60.3
b	392	(65.5)
4a	328	(69.5)
b	240	56.1
5a	515	34.3
b	847	74.0
6	442	49.9
7	300	48.1
8	380	(49.4)
9	517	42.7
Mean	417	51.9
±SD	153	13.0

Parentheses indicate three studies in which the computer was unable to find a unique solution for β'.
* Calculated from κ', the TCER. $T_{1/2}$ is the time taken for plasma [^{113m}In]Tf to reach one-half of the value at t_0.
‡ Calculated using Eqs. 7 and 8. $t_{1/2}$ is the time taken for the mass of [^{113m}In]Tf in the pulmonary interstitium to equal one-half the mass present when the net exchange of tracer between vascular and lung interstitial compartments becomes equal to zero.

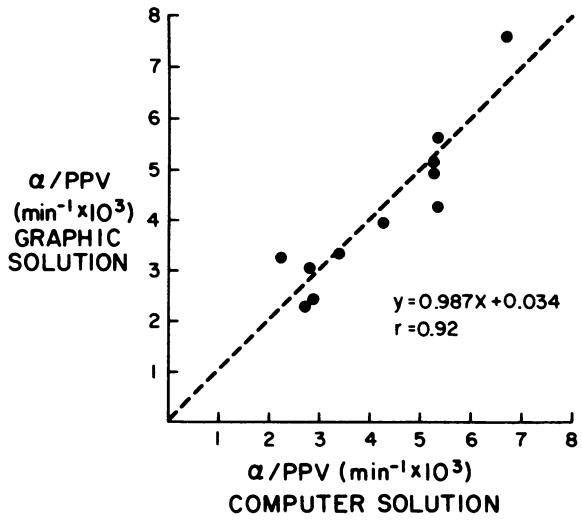

FIGURE 7 Correlation of values of the pulmonary transcapillary escape rate (α/PPV) calculated from a single measurement using two different methods. α/PPV determined by an iterative process (computer solution) is shown on the abscissa. α/PPV determined by a simple graphic technique on the ordinate.

and Vc in these normal subjects are consistent with those reported by other investigators (15–18). The mean value of α_T, 10.6 ml/h or 0.0029 ml/s is very close to that we reported in sheep 0.0027 ml/s (8). The pulmonary transcapillary escape rate (α/PPV) in man is twofold greater than TCER. This is seen even though convective forces driving transvascular flux in the lung are smaller than those seen in the peripheral microvessels. The finding is compatible with either greater "porosity", or greater surface area/unit volume of exchanging vessels in the lung when compared to the vascular bed of the body as a whole. Studies of transendothelial flux of macromolecules in other species (sheep, mouse, rabbit, dog) also indicate that vascular permeability is much greater in lung than in tissues such as skin and muscle (which comprise the majority of body mass) (11, 12, 19, 20).

The $t_{1/2}$ is very much shorter in man than the $t_{1/2}$ measured in sheep lung (man, 52 min; sheep, 151 min) (8). Using average values of β' and κ' in Eq. 8, indicates that steady-state exchange between IV and EV compartments is reached between 3.5–4 h after intravenous bolus administration of [^{113m}In]Tf. Equally rapid equilibration of tracer albumin has been reported in mouse lung and rat lung (12, 19, 21).

We have previously discussed sources of variability or error in measurement of pulmonary transvascular protein flux by the external radioflux detection method (8). Two areas require additional discussion in the light of the present data.

(*a*) We assumed that all externally detected radioactivity originates in lung. Actually, both isotopic markers are widely distributed. We have contended that because this noninvasive method is sensitive to the rate at which ^{113m}In counts accumulate in the EV space, rather than the absolute count rate, it will be little affected by the slow flux of macromolecules into chest wall tissue. This argument is more valid given the very rapid $t_{1/2}$ for tracer equilibration seen in human lung.

Additionally, we have now studied subjects using both a focused collimator, designed to minimize detection of counts arising in the chest wall, and "wide-open" collimators. In Fig. 8 we compare measurements of α(normalized to PBV) in five normal subjects, made at an interval of at least 6 mo, using a single-channel collimator on the first occasion, and the focused collimator on the second occasion. Four studies obtained in patients are also shown. Here, measurements were simultaneously made over the right midlung field and the left lung apex. Intervening soft tissues varied greatly between these regions. Both in normals and in patients, the paired values are comparable. This indicates a lack of major data input from the chest wall during the first

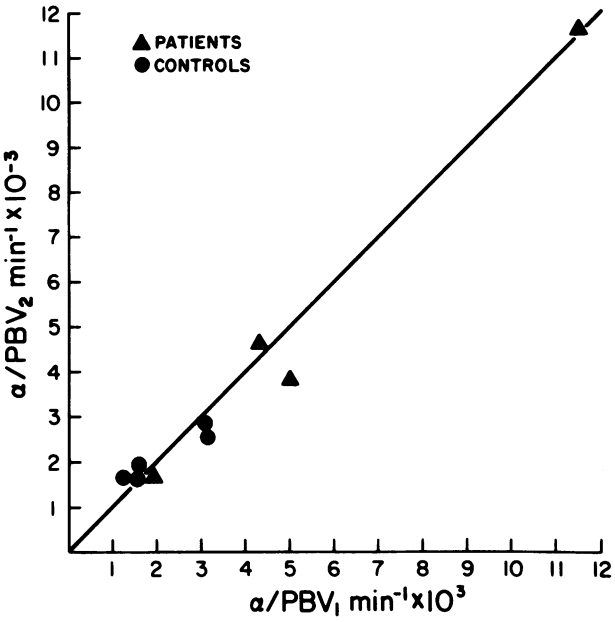

FIGURE 8 Correlation of replicate measurements of α (normalized to PBV). In control subjects, the measurements were made at an interval of at least 6 mo. The first measurement (abscissa) was made using a single-channel, diverging collimator. The second measurement was made using a multihole focussed collimator. In the four patient studies, probes with single-channel diverging collimators were placed over a right and a left lung field, and the two measurements were obtained simultaneously. One patient (α/PBV ~ 5) had congestive heart failure, and the final patient had a bronchopneumonia. The line drawn is that of identity.

60 min of study, and is also an index of the reliability of this measurement. We now recommend use of a multi-hole parallel channel collimator to adequately limit the field of view of the detector laterally, while still retaining a very high sensitivity (high geometric efficiency).

(*b*) We extrapolate from measurements made in a small core of lung tissue to events occurring in the entire lung. Obviously, extension from part to whole depends on the homogeneity of transvascular protein flux across the lung. We studied subjects supine, rather than upright, to minimize zonal effects in the distribution of perfusion to lung regions (22, 23).

A graphic method has been used both to extrapolate from regional to whole organ data, and to estimate regional parameters (α and β') in a small group of studies which could not be analyzed using the customary iterative process. We have shown that in normal subjects the graphic method yields a good estimate of α for the region being sampled. The actual value of the computed α_T depends largely on the assumed volume of the vascular compartment in the lung exchanging with the interstitial space. We used Vc in our calculations because this could be independently measured in each subject. Vc determined by the method of Roughton and Forster, 1957, may vary from anatomic pulmonary Vc (measured morphometrically) by a factor of 2 (24). Presumably, this relates to areas of the lung that are not ventilated but are either perfused or have static blood volumes (25). Although it is unlikely that static blood volume would be a site of transvascular protein flux, use of Vc may lead to systematic underestimation of the intravascular exchanging volume, and thus a systematic error in the extrapolation to α_T. This is difficult to assess in the absence of direct access to lung lymph in man.

The coefficient of variation in measurements of α_T (between subjects) was 0.48. This is greater than that noted in sheep (0.23). In our animal studies, measurements were made using the same collimator-detector unit in every case, and sampling a small core of tissue in exactly the same location in each sheep. Calculation of the whole lung parameter for α involved an assumed compartment volume. In man, extrapolation from regional to whole lung data combines the variability of external radioflux detection with the variability of Vc determination. Measurement of pulmonary transcapillary escape rate, α/PPV, involving only external radioflux detection, had a coefficient of variation of 0.39. This variability may in part be attributed to the variety of collimator-detector units used in making these measurements, and to some regional variation in transvascular protein exchange.

In sheep, endothelial injury in the lung typically causes at least a two- to threefold increase in transvascular protein flux (5, 8, 26). Yet, significant pulmonary edema is rarely seen with an insult of this magnitude (26). Presumably, even a greater increase in transendothelial protein flux must occur before the "pulmonary edema safety factors" in lung are overwhelmed. Thus, the sensitivity of external radioflux detection in man is such that it should detect all clinically significant changes in pulmonary transvascular protein flux.

We have used external radioflux detection to measure pulmonary transvascular protein flux in man. The method is minimally invasive, and in our recent studies, using the ADAC probe, total radiation dose to the subject is only 115 mrad. We have demonstrated the validity of the method in suitable animal models (8). In 1979, Prichard and Lee (27) successfully used a similar approach to assess vascular permeability in the dog lung. Although the actual value of α will vary with placement of the detector, or the specific detectors used, we have described two means of normalizing data which makes possible comparisons of data obtained in different laboatories or clinical facilities. Measurement of pulmonary transvascular protein flux in human disease states may be useful in clinical investigation and patient management.

APPENDIX

We have found that the graphic method (subtraction of D_{EVe} from D_{IV}) yields a poor estimate of β'. The reason for this is easily demonstrated:

$$[D_{IV}]_{t_i} = [D_{IV}]_{t_o} e^{-\kappa' t_i}. \quad (3)$$

The equilibration of tracer between plasma and lymph in a simple two-compartment system is commonly expressed as,

$$[D_{IV}]_{t_i} - [D_{EV}]_{t_i} = [D_{IV}]_{t_o} e^{-ut_i}. \quad (12)$$

Subtracting Eq. 12 from Eq. 3, we obtain,

$$[D_{EV}]_{t_i} = [D_{IV}]_{t_o} (e^{-\kappa' t_i} - e^{-ut_i}). \quad (13)$$

Multiplying both sides of the equation by V_{IS} we obtain,

$$D_{EV_{t_i}} = [D_{IV}]_{t_o} V_{IS} (e^{-\kappa' t_i} - e^{-ut_i}). \quad (14)$$

This is similar in form to Eq. 7,

$$D_{EV_{t_i}} = [D_{IV}]_{t_o} \frac{\alpha}{\beta' - \kappa'} (e^{-\kappa' t_i} - e^{-\beta' t}).$$

Thus, if $u = \beta'$, $\alpha/(\beta' - \kappa') = V_{IS}$, and $\alpha/(\beta' - \kappa') \neq Vp$. The graphic solution will only yield a reasonable estimate of β' when $Vp \simeq V_{IS}$.

ACKNOWLEDGMENT

This study was supported by a grant from the National Heart, Lung, and Blood Institute (HL19155), Pulmonary Edema Specialized Center for Research.

REFERENCES

1. Staub, N. C. 1974. Pulmonary edema. *Physiol. Rev.* **54:** 678–811.
2. Brigham, K. L., J. D. Snell, Jr., T. R. Harris, S. Marshall, J. Haynes, R. E. Bowers, and J. Perry. 1979. Indicator dilution lung water and vascular permeability in humans: effects of pulmonary vascular pressure. *Circ. Res.* **44:** 523–530.
3. McNamee, J. E., and N. C. Staub. 1979. Pore models of sheep lung microvascular barrier using new data on protein tracers. *Microvasc. Res.* **18:** 220–244.
4. Erdmann, A. J., III, T. R. Vaughan, Jr., K. L. Brigham, W. C. Woolverton, and N. C. Staub. 1975. Effect of increased vascular pressure on lung fluid balance in unanesthetized sheep. *Circ. Res.* **37:** 271–284.
5. Brigham, K. L., R. E. Bowers, and J. Haynes. 1979. Increased sheep lung vascular permeability caused by *Escherichia coli* endotoxin. *Circ. Res.* **45:** 292–297.
6. Anderson, R. R., R. L. Holliday, A. A. Driedger, M. LeFcoe, B. Reid, and W. J. Sibbald. 1979. Documentac tion of pulmonary capillary permeability in the adult respiratory distress syndrome accompanying human sepsis. *Am. Rev. Respir. Dis.* **119:** 869–877.
7. Vreim, C. E., and N. C. Staub. 1976. Protein composition of lung fluids in acute alloxan edema in dogs. *Am. J. Physiol.* **230**(2): 376–379.
8. Gorin, A. B., W. J. Weidner, R. H. Demling, and N. C. Staub. 1978. Noninvasive measurement of pulmonary transvascular protein flux in sheep. *J. Appl. Physiol.* **45**(2): 225–233.
9. Korubin, V., M. N. Maisey, and P. A. McIntyre. 1972. Evaluation of technetium-labeled red cells for determination of red cell volume in man. *J. Nucl. Med.* **13:** 760–762.
10. Parving, H. H., N. Rossing, S. L. Nielsen, and N. A. Lassen. 1974. Increased transcapillary escape rate of albumin, IgG, and IgM after plasma volume expansion. *Am. J. Physiol.* **227**(2): 245–250.
11. Wittmers, L. E., Jr., M. Bartlett, and J. A. Johnson. 1976. Estimation of capillary permeability coefficients of inulin in various tissues of the rabbit. *Microvascular Res.* **11:** 67–68.
12. Studer, R., and J. Potchen. 1971. The radioisotopic assessment of regional microvascular permeability to macromolecules. *Microvasc. Res.* **3:** 35–48.
13. Snedecor, G. W., and W. G. Cochran. 1967. Statistical Methods. Iowa State University Press, Iowa City, Iowa.
14. Roughton, F. J. W., and R. E. Forster. 1957. Relative importance of diffusion and chemical reaction rates in determining rate of exchange of gases in the human lung, with special reference to true diffusing capacity of the pulmonary membrane and volume of blood in the lung capillaries. *J. Appl. Physiol.* **11:** 290–302.
15. Wochner, R. D., M. Adatepe, A. VanAmburg, and E. J. Potchen. 1970. A new method for estimation of plasma volume with the use of the distribution space of indium-113m-transferrin. *J. Lab. Clin. Med.* **75**(5): 711–720.
16. van der Merwe, E. J., M. G. Lotter, P. D. R. van Heerden, C. F. Slabber, and J. Bester. 1970. Absorbed dose calculations for 113mIn placental scanning. *J. Nucl. Med.* **11:** 31–35.
17. Daly, W. J., S. T. Giammona, and J. C. Ross. 1965. The pressure-volume relationship of the normal pulmonary capillary bed. *J. Clin. Invest.* **44**(7): 1261–1269.
18. Georges, R., G. Saumon, and A. Loiseau. 1978. The relationship of age to pulmonary membrane conductance and capillary blood volume. *Am. Rev. Respir. Dis.* **117:** 1069–1078.
19. Studer, R. K., J. Morgan, M. Penkoske, and E. J. Potchen. 1973. Regional vascular volume and extravascular accumulation of labeled protein during plasma volume expansion. *Am. J. Physiol.* **224**(3): 699–704.
20. Renkin, E. M. 1978. Transport pathways through capillary endothelium. *Microvasc. Res.* **15:** 123–135.
21. Nicolaysen, G., and N. C. Staub. 1975. Time course of albumin equilibration in interstitium and lymph of normal mouse lungs. *Microvasc. Res.* **9:** 29–37.
22. West, J. B. Ventilation/Blood Flow and Gas Exchange. 1965. Blackwell Scientific Publications, Oxford, England.
23. Daly, W. J. 1969. Pulmonary diffusing capacity for carbon monoxide and topography of perfusion during changes in alveolar pressure in man. *Am. Rev. Respir. Dis.* **99:** 548–553.
24. Weibel, E. R. 1963. Morphometry of the Human Lung. Academic Press, Inc., New York.
25. Vreim, C. E., and N. C. Staub. 1973. Indirect and direct pulmonary capillary blood volume in anesthetized open-thorax cats. *J. Appl. Physiol.* **34**(4): 452–459.
26. Brigham, K. L., W. C. Woolverton, L. H. Blake, and N. C. Staub. 1974. Increased sheep lung vascular permeability caused by pseudomonas bacteremia. *J. Clin. Invest.* **54:** 792–804.
27. Prichard, J. S., and G. de J. Lee. 1979. Measurement of water distribution and transcapillary solute flux in dog lung by external radioactivity counting. *Clin. Sci.* **57:** 145–154.